



ELSEVIER

Contents lists available at ScienceDirect

# Solar Energy Materials & Solar Cells

journal homepage: [www.elsevier.com/locate/solmat](http://www.elsevier.com/locate/solmat)

## Advanced microhole arrays for light trapping in thin film silicon solar cells



Daniel Lockau<sup>a,c,\*</sup>, Tobias Sontheimer<sup>a</sup>, Veit Preidel<sup>a,b</sup>, Florian Ruske<sup>a</sup>,  
Martin Hammerschmidt<sup>c</sup>, Christiane Becker<sup>b</sup>, Frank Schmidt<sup>c</sup>, Bernd Rech<sup>a</sup>

<sup>a</sup> Helmholtz-Zentrum Berlin für Materialien und Energie, Institute for Silicon Photovoltaics, Kekuléstr. 5, D-12489 Berlin, Germany

<sup>b</sup> Helmholtz-Zentrum Berlin für Materialien und Energie, Young Investigator Group Si-Nanoarchitectures, Kekuléstr. 5, D-12489 Berlin, Germany

<sup>c</sup> Zuse-Institut Berlin, Takustr. 7, D-14195 Berlin, Germany

### ARTICLE INFO

Available online 3 December 2013

#### Keywords:

Photovoltaics  
Light trapping  
Nano-optics  
Simulation  
FEM

### ABSTRACT

We present a comprehensive theoretical analysis accompanying our experimental development of microstructured thin film polycrystalline silicon solar cell absorbers. Our focus is on 2D-periodic arrays of holes which do not act as a superficial scattering grating but pierce the entire silicon absorber layer. We deviate from the commonly used model of vertical hole sidewalls by employing conical frustum shaped holes with a range of opening angles. Additionally, an experimentally motivated front texture is applied to the simulated solar cell absorbers and varied in texture aspect. Based on this parametric absorber model, for a single domain period of 2  $\mu\text{m}$ , we discuss light trapping and optical losses in thin film cells with absorptive front and back contacts and a perfectly transparent glass encapsulation layer. Implications from this study are that light trapping in square periodic arrays with periods larger than the wavelength of light can be enhanced by microholes but that it cannot replace a front texture which provides both antireflection and scattering.

© 2013 Elsevier B.V. All rights reserved.

### 1. Introduction

Periodic arrays of holes have been suggested by several groups as dielectric light trapping structures in thin film silicon photovoltaics. These structures can serve as a diffraction grating at the surface of a silicon absorber medium [1], a configuration for which high absorption enhancement factors have been predicted under particular circumstances [2]. Another possible implementation is holes that pierce the entire absorber layer, a geometric layout which is commonly seen as an alternative to the nano-pillar or nano-wire concept. The wire concept has the electrical benefit of allowing a charge collection with even lower diffusion path lengths [3] but considering the light trapping it has been reported by several groups that nanoholes can be more efficient than nano-pillar concept [4,5]. Modifications of the hole and pillar structures in terms of variable diameter, height, period and also non-vertical sidewalls have already been tested for nanoholes [6,7] and nano-pillars [8,9]. The publications report on improved antireflection properties and better light trapping due to a higher number of modes when comparing non-vertical to vertical sidewalls.

All of the publications cited above treat periodic geometries with periods below 1  $\mu\text{m}$ , but experimental geometries previously produced in our laboratories feature strong absorption for periods

$\geq 2 \mu\text{m}$  [10,11]. For these structures we were able to show, by optical simulation, that the microhole array which can be derived from the experimentally fabricated silicon microstructure [12] had superior light trapping properties in the presence of a lossy transparent conductive oxide layer than the initially deposited silicon microdome array [13,14]. The increased optical performance was partly attributed to reduced parasitic absorption in a flat rear contact configuration. In this contribution, we extend the analysis of conical frustum microhole arrays with 2  $\mu\text{m}$  domain period by using a parametric model instead of experimentally given absorber geometries. By optimizing microhole geometry parameters and evaluating the importance of front texturing for microhole structured absorbers, we present possible benefits of the microhole structure for the optics in thin film solar cells and provide a simulation-aided approach for the design of novel structures with tailored optical properties.

### 2. Materials and methods

#### 2.1. Simulation setup

We base this study on few micrometer thick arrays of microholes with non-vertical sidewalls, which have been fabricated on patterned solgel substrates. Two experimentally realized structures, one (i.) on a U-shaped substrate and the other on a mostly planar substrate with cylindrical pillars (ii.), which were produced using electron beam evaporation and solid phase crystallization

\* Corresponding author.

E-mail address: [daniel.lockau@helmholtz-berlin.de](mailto:daniel.lockau@helmholtz-berlin.de) (D. Lockau).

[10] are depicted in Fig. 1(a). The light trapping of the geometry (i.) upon inclusion into a solar cell stack of an absorptive front transparent conductive oxide (TCO), silicon absorber and back TCO/silver reflector was studied in Refs. [13,14]. The simulated solar cell layouts from these publications are included in the solar cell model depicted to the right in Fig. 1(b). In this contribution, we substitute the experimental absorber texture by a parametric model but retain the previously used solar cell structure model: The front TCO thickness is 300 nm, assuming a strictly vertical growth. Back TCO thickness is 85 nm. Microholes in the absorber are filled with glass. The solar cell is assumed to be illuminated through a thick glass layer without antireflection coating. We assumed a glass height of 1 mm for computation according to Eq. (2).

The parametric model absorber, which we employ for the simulations in this paper, is depicted in Fig. 1(c). Fixed parameters are the texture period " $p$ " ( $2\ \mu\text{m}$ ) and the height " $h$ " ( $2.4\ \mu\text{m}$ ) of the conical frustum holes. Open parameters are the hole central radius " $r_{0.5h}$ ", the sidewall angle " $\alpha$ " and the parameter " $d_{\text{front}}$ ", describing the maximum amplitude of a front texturing which was fitted to the substrate morphology of the previously studied experimental structure [13]. The grid shown in Fig. 1(c) depicts a parameter setting with  $d_{\text{front}}=600\ \text{nm}$ . A detailed description of how the surfaces are constructed is given in A.2).

All simulations were performed using a refractive index of 1.47 for glass. Standard bulk refractive index and extinction coefficient values, tabulated by Palik [15], were used for the silver reflector. Our silicon data set is a crystalline silicon data set, very similar to the one tabulated by Palik, but with a higher sampling point density close to the band edge. As TCO material we employ a high mobility Aluminum-doped Zinc Oxide (ZnO:Al) model. The model was obtained by fitting a model dielectric function comprising a Leng oscillator to describe band gap absorption and a Drude oscillator with frequency-dependent damping [16] to optical measurements on a high-quality ZnO:Al sample with low free carrier concentration and high carrier mobility [17].

Maxwell's equations were solved on space discretized versions of the unit cell computational model – a sample discretization of the silicon volume is depicted in Fig. 1(c) – using the finite element package JCMsuite [18]. Lateral boundary conditions were chosen periodic and transparent perfectly matched layer (PML) boundary conditions were applied to bottom and top boundary surfaces. For

illumination, a normally incident plane wave in  $+z$ -direction, referring to the setup in Fig. 1(b), was used in all simulations. Absorbance integrals and scattered intensity were computed from the obtained solutions. Computational errors of all results should be smaller than 2% of the incident irradiance at wavelengths below 700 nm and smaller than 1% at higher wavelengths. High accuracy solutions were assured for the computation of light path enhancement in the wavelength range longer 1000 nm. To take the additional light trapping into account which is provided by the glass encapsulation, the finite element model was incoherently coupled to a glass layer for simulation as described below.

## 2.2. Coupling of the glass layer

The monochromator bandwidth of the thermal light sources employed for quantum efficiency measurement usually is of a few nanometers. When considering such a light source, the rigorous solution to Maxwell's equations computed at a single wavelength point is still valid but an incoherent averaging needs to be carried out over a characteristic ensemble of states to obtain results which are comparable to the experiment. This can be achieved rigorously but with high computational effort by computing the incoherent average over the bandwidth of the light source. To estimate the contribution of the glass encapsulation to light trapping, we substitute the computationally expensive rigorous procedure by a simple algorithm motivated by the decoupling of two scale separated operators in the 1D case. The motivation can be best explained by considering the domain coupling in terms of the additive Schwarz iteration [19,20]:

In the two domain case, the Schwarz iteration is started from the decoupled case and keeps adding scattered fields of the subdomains to the incoming field of the respective other subdomain until a desired level of convergence is reached. In a homogeneous medium, the fields can be realized as vectors of Fourier coefficients, representing the Fourier decomposition of the outward radiating field of each sub-domain. In the following the two subdomains will be denoted by subscripts 1, 2, iterations will be denoted by superscripts in braces. The two linear operators calculating the scattered field of a subdomain towards the other subdomain will be denoted by  $A_{1,2}$ . The initially incoming fields are denoted by  $i_{1,2}$  and the scattered fields in iteration  $n$  by  $u_{1,2}^{(n)}$ .

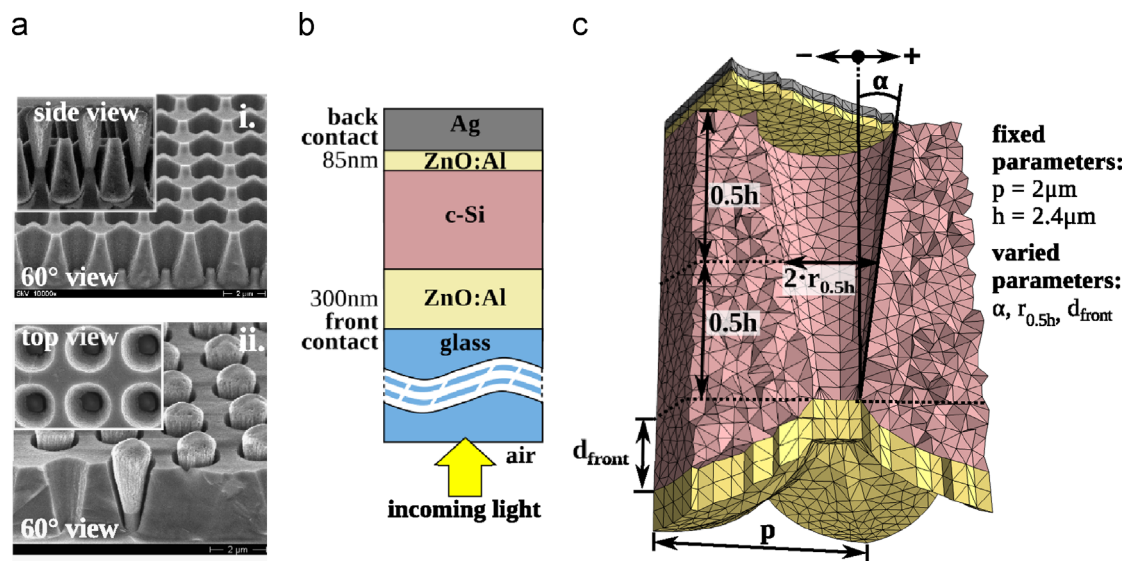


**Fig. 1.** (a) Silicon structures fabricated by electron beam evaporation, solid phase crystallization and selective etching on U-shaped (i.) and mostly flat (ii.) substrates. Periods of the geometry are  $2\ \mu\text{m}$  (i.) and  $2.35\ \mu\text{m}$  (ii.) in lateral directions. The conical tips visible in i. (inset) can be removed to produce a microhole array as shown in i. and ii. (inset), (b) vertical device structure of the solar cell model. Highly doped silicon layers were not included into the cell model and (c) parametric silicon absorber model used for the simulations in this publication.

Download English Version:

<https://daneshyari.com/en/article/78116>

Download Persian Version:

<https://daneshyari.com/article/78116>

[Daneshyari.com](https://daneshyari.com)